

PAPER

87 fs CEP-stable Cr:ZnSe laser system

To cite this article: Pavel Komm *et al* 2018 *Laser Phys.* **28** 025301

View the [article online](#) for updates and enhancements.

87 fs CEP-stable Cr:ZnSe laser system

Pavel Komm¹, Uzziel Sheintop^{1,2}, Salman Noach² and Gilad Marcus¹

¹ Department of Applied Physics, Benin School of Engineering and Computer Science, Hebrew University of Jerusalem, Jerusalem 9190401, Israel

² Department of Applied Physics, Electro-Optics Engineering Faculty, Jerusalem College of Technology, Jerusalem 91160, Israel

E-mail: gilad.marcus@mail.huji.ac.il

Received 3 November 2017

Accepted for publication 14 November 2017

Published 22 January 2018



Abstract

A hybrid laser scheme for the generation and amplification of mid-IR ultrashort pulses, with a carrier to envelope stable phase, is presented. Seed mid-IR pulses with picojoule energies are obtained via intrapulse difference frequency generation from an 8 fs Ti:sapphire oscillator. The energy of these seed pulses is then amplified in a multipass Cr:ZnSe laser amplifier to more than a nanojoule/pulse level. The duration of the amplified impulses is measured to be 87 fs, and the width of their spectrum supports their compression to ~50 fs.

Keywords: infrared laser, Cr:ZnSe, CEP stable, femtosecond laser

(Some figures may appear in colour only in the online journal)

Trains of attosecond bursts of light are presently attainable through high harmonics generation (HHG) [1, 2]. However, to produce isolated single attosecond pulses for time-domain spectroscopy, it is crucial to lock the carrier to envelope phase (CEP) of the HHG driving laser [3–5]. With current technology, which is mainly based on Ti:Sapphire lasers that work at a carrier wavelength of ~800 nm, the HHG photon-energies are limited to ~150 eV. However, many applications will benefit from much higher photon-energies, extending into the soft x-ray [6]. The Process of HHG is easily understood within the framework of the well-known three-step model of HHG [7, 8]. According to this model, the cutoff energy of the high harmonics spectrum scales with the square of the carrier wavelength of the HHG driving light source [9–12]. Thus, a laser drive with a longer wavelength would be able to produce HHG with more energetic photons. Here we report on a CEP stable laser system with a carrier wavelength of ~2450 nm.

In the past, due to the lack of laser materials with a broad enough gain spectrum in the infrared, optical parametric amplifiers (OPAs) and optical parametric chirped pulse amplifiers (OPCPAs) were the only alternatives for the generation of ultrashort pulses in this spectral range. OPAs and OPCPAs have in some cases broad gain-bandwidth [13–15], they exhibit high gain, and usually, thermal load is not an issue. In addition, a major advantage of OPAs and OPCPAs is their ability to passively lock the CEP of the amplified pulse through the nonlinear process of difference frequency generation (DFG) [15–17].

Besides their many advantages, OPAs and OPCPAs also have their disadvantages: (a) they need an expensive and complicated ultrafast pump laser with pulse durations below few picoseconds, (b) the seed and the pump must be synchronized to a sub-picosecond accuracy, and (c) due to the phase matching conditions, their spectrum is very sensitive to pointing instabilities.

The unfortunate situation of unavailability of large gain-bandwidth laser materials in the infrared is now changing [18–23]. Particularly attractive for ultrafast pulse generation and amplification are the divalent chromium-doped chalcogenides, specifically Cr:ZnSe and Cr:ZnS. These materials have an extensive gain bandwidth (>500 nm), which perfectly overlap the atmospheric transparency window between 2 and 2.5 μm in the mid-IR. Moreover, they can be conveniently pumped by commercially available Tm: fiber and Er: fiber lasers, as well as solid-state lasers, such as 1.9 μm Tm:YLF. In fact, the spectroscopic and thermal properties of Cr:ZnSe echo those of the ubiquitous Ti:sapphire to such an extent that it is sometimes called ‘Ti:sapphire of the mid-IR’ [24].

The swift evolution of ultrafast Cr:ZnSe and Cr:ZnS lasers in the past decade may indeed facilitate their implementation as high harmonics generating femtosecond light sources. In 2006, Sorokina *et al* have demonstrated femtosecond Cr:ZnSe laser operation for the first time. Their SESAM mode-locked oscillator generated ~100 fs pulses at 75 mW of output power, around 2.45 μm [25]. A long-standing record of 80 fs for Cr:ZnSe out of the oscillator pulse duration was set the

following year by the same group [26]. Even shorter, 41 fs, pulses were obtained from a graphene mode-locked oscillator incorporating Cr:ZnS as the gain medium [27]. Recently, a 29 fs, 4.4 nJ/pulse mid-IR Kerr-lens mode-locked polycrystalline Cr:ZnS laser was reported by Vasilyev and colleagues [28].

Despite the impressively rapid recent progress in the field of Cr²⁺ doped II–VI semiconductor ultrafast lasers, the issue of their CEP stability, pivotal from the point of view of HHG and frequency combs communities, has not been addressed yet [29]. Here we propose and demonstrate a hybrid amplification scheme in which, at the first stage we generate infrared CEP locked seed pulse through intra-pulse DFG from an 8 fs commercial Ti:sapphire oscillator. The seed is next amplified in a multistage Cr:ZnSe amplifier which is pumped by a Q-switched Tm:YLF laser.

A paradigm, whereby parametric seed generation and its laser amplification are implemented in tandem, preserves the advantage of passively stabilizing the CEP of the signal through intrapulse DFG and benefits from the simplicity of its laser amplification. Such a scheme was recently proposed and demonstrated by Potemkin *et al* for yet another transition metal doped II–VI semiconductor gain medium, specifically Fe²⁺:ZnSe, which has its gain spectrum deeper in the mid-IR, at the 4–5 μm spectral region [30–32].

Figure 1(a) presents a sketch of the experimental arrangement. The output of our 80 MHz mode-locked Ti:Sapphire laser (Venteon: Pulse one) is temporally pre-compressed in a BK7 prism-pair compressor and focused by an off-axis parabolic mirror, with an effective focal length of 15 mm, into 1 mm thick periodically poled Lithium Niobate (PPLN) crystal (Raicol Crystals Ltd), with a polling period of 16 μm . The spectrum of our mode-locked Ti:Sapphire laser is shown in figure 1(b). At the bottom of figure 1, i.e. in figure 1(c), we show the phase matching curves for the DFG process in the PPLN. A single pass through the non-linear crystal produces ~ 1 pJ mid-IR seed pulse-train at 80 MHz. After the parametric generation in the crystal, the seed beam is collimated with a second off-axis parabolic mirror, identical to the first one. Prior to the injection into the Cr:ZnSe amplifier, the repetition rate of the seed pulse train is reduced to 1 kHz, using an RTP pulse picker (FastPulse Technology, Inc.), and synchronized with the pump laser.

A homebuilt actively Q-switched Tm:YLF laser, operated at 1 kHz serves as the optical pump source. It is based on a previously described passively Q-switched Tm:YLF design [33], in which the passive saturable absorber Q-switch was replaced by an active acousto-optic Q-switch (Gooch and Housego). The gain medium of this laser is end-pumped by a continuous-wave diode at 793 nm, resulting in a slope efficiency of 44.7%, pulse energy of 1.6 mJ/pulse, pulse duration of ~ 70 ns FWHM, at a central wavelength of 1886 nm.

About 380 microjoules/pulse of the pump laser output were aimed at a Brewster angle and focused to a spot-size of 60 μm (FWHM) in the CrZnSe crystal. The pump absorption in the 7 mm long crystal was measured to be 86%. The seed pulses were focused by the first concave spherical mirror of the amplifier (gold coated, $f = 100$ mm, marked as CM1 in

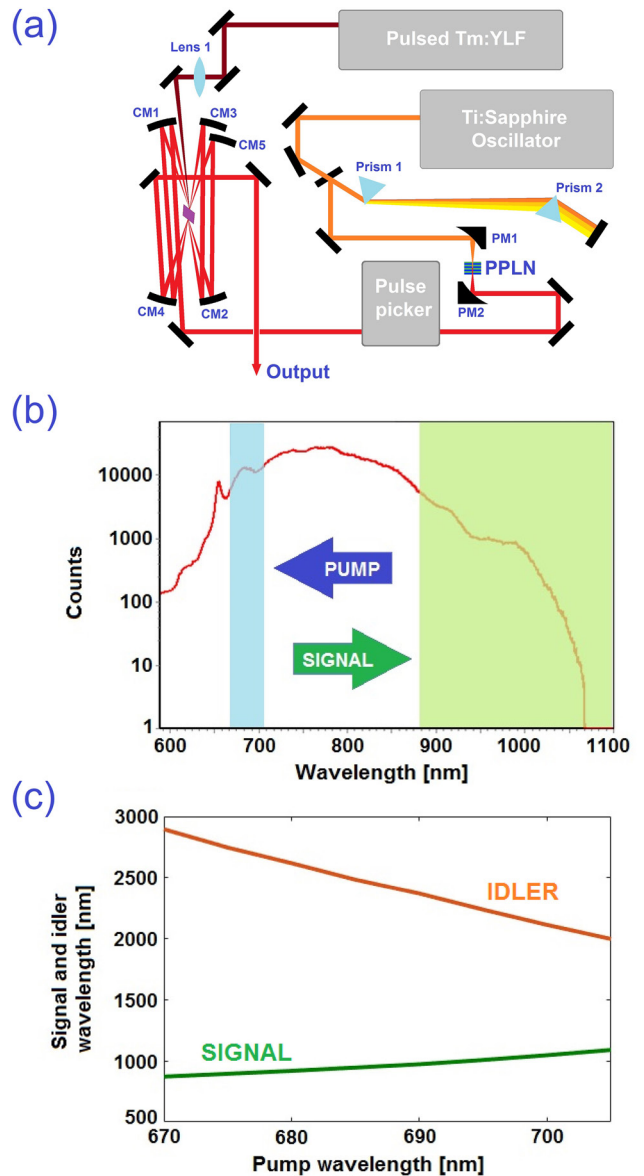


Figure 1. (a) A scheme of the Cr:ZnSe laser system. Prisms 1 and 2 comprise the chirp compensating compressor for the Ti:Sapphire mode-locked laser output. Here PPLN stands for periodically poled lithium niobate and PM(1,2) are the $f = 1.5$ cm parabolic mirrors. The curved mirrors of the four-pass amplifier, with $f = 10$ cm, are designated CM(1–4) and the fifth mirror with $f = 7.5$ cm is CM5. Lens 1 is the $f = 25$ cm pump focusing lens. (b) The spectrum of the mode-locked Ti:Sapphire oscillator. Pump and signal spectral regions which are subtracted from one another in the DFG process are highlighted in blue (pump) and green (signal). (c) The phase matching curves for the Ti:Sapphire intrapulse DFG process in 16 μm PPLN. The orange (top) and the green (bottom) curves represent the idler and the signal wavelengths respectively.

figure 1), and directed by it, to spatially overlap with the pump in the Cr:ZnSe crystal. The amplifier itself consists of additional three concave spherical mirrors, identical to the first one (CM2, CM3 and CM4 in figure 1) and a fifth mirror (CM5 silver coated, $f = 75$ mm). The latter allows to independently control the overlap of the amplified seed with the pumped volume in the gain medium, at its fourth and final passage through it.

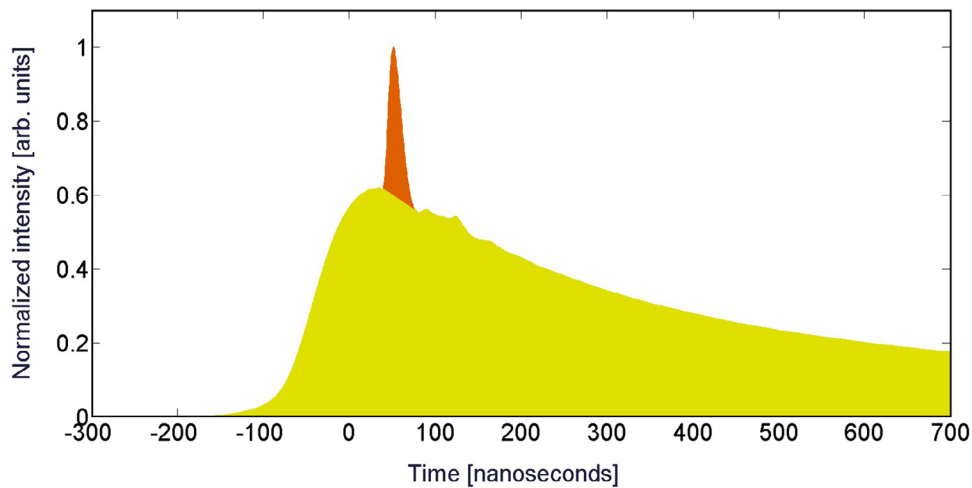


Figure 2. A single amplified MIR ultrashort pulse (orange) on top of ASE pedestal (yellow), as measured with the PDA10D detector.

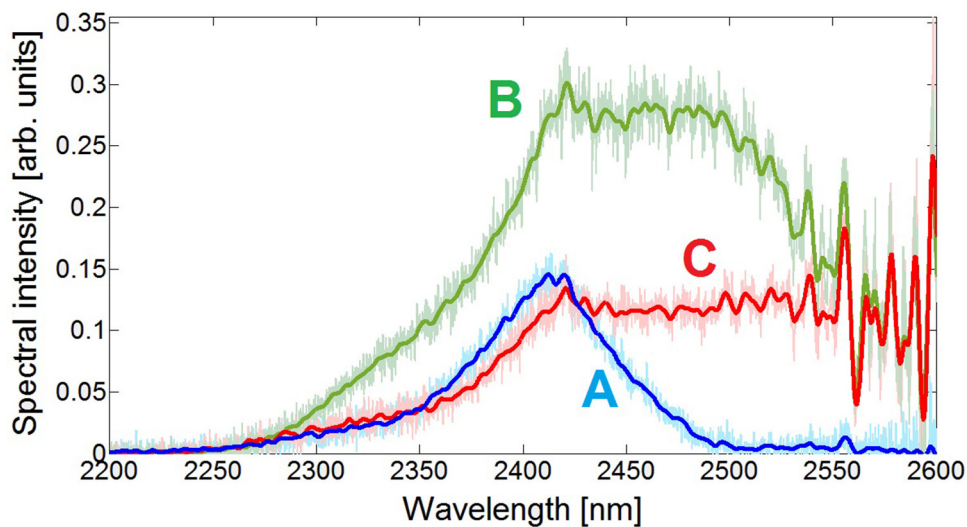


Figure 3. Three spectra of the amplified signal, each measured with different amount of insertion of the second prism of the compressor, i.e. prism 2 in figure 1(a). In all the three spectra, the thin faint lines represent the raw data points, and the thick lines are the local moving averages of the raw data. Spectrum C was measured with the prism inserted by 0.785 mm, from its middle position, at which spectrum B was measured, while spectrum A was taken with the prism retracted by 0.535 mm, from the middle position.

At the completion of the four passes, the average energy of a single IR pulse, including both the amplified signal and the amplified spontaneous emission (ASE) was measured by a laser power meter and found to be ~ 60 nJ/pulse. To evaluate the energy ratio between the amplified seed and the ASE we used a photodiode (Thorlabs PDA10D: 15 MHz bandwidth, ~ 23 ns rise time) to record the output of the amplifier, as a function of time. Figure 2 shows the recorded waveform, in which the amplified single ultrashort pulse is clearly visible on top of the much slower ASE intensity envelope. A single pulse selection was guaranteed by a narrow, 5 ns long, temporal gating of the pulse picker. The ratio of the amplified seed energy to the ASE energy was assessed, by calculating the brown to yellow area ratio in figure 2, and was found to be roughly 1:50. The calculation was performed while including the long decay tail of the ASE at later times, which is not shown in figure 2. Evidently, more than 1.1 nJ/pulse of signal energy is attained after four passes in the amplifier, a value comparable

to a single pulse energy of a typical Cr:ZnSe ultrafast oscillator output, but with the benefit of CEP stability.

To measure the spectrum of the output, we used a scanning monochromator (GCA/McPherson) and the abovementioned PDA10D photodetector. The measured spectra, corrected for the responsivity of the detector, can be seen in figure 3. A degree of control over the seed spectrum is provided by the prism-pair compressor, as is evident from the three spectra of the amplified signal, each taken at a different amount of insertion of the second prism (prism 2 in figure 1(a)).

We would like to stress the fact that all the three spectra presented here are of the amplified seed only, excluding ASE. It was straightforward to separate between signal and ASE contributions while recording waveforms like the one shown in figure 2, for each of the spectral components of the output beam. The amplitude of the amplified signal impulse was measured in each one of the recorded waveforms and plotted as a function of wavelength, to construct the spectra seen in figure 3.

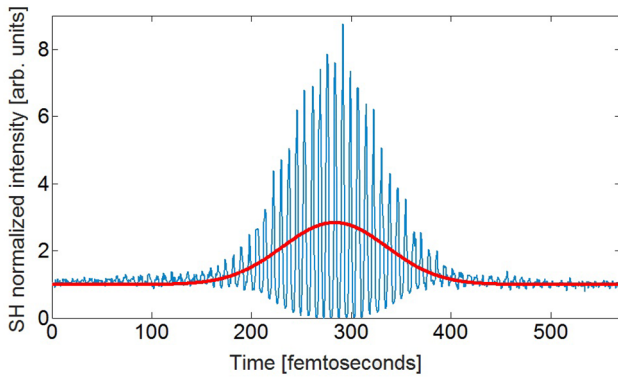


Figure 4. Interferometric autocorrelation of the Cr:ZnSe amplifier output is presented by the blue curve. The thick (red) curve is the Gaussian fit of the intensity autocorrelation, indicating a pulse width of 87 fs FWHM.

Spectrum B is characteristic of the 1.1 nJ/pulse output. It is roughly 175 nm wide, and its Fourier transform (FT) produces a ~ 50 fs long pulse (intensity envelope FWHM). It was easy to extend and broaden the signal spectrum towards longer wavelengths by inserting the second prism (spectrum C, figure 3), at the expense of pulse energy. Retracting the prism though, produced little if any spectral shift to the blue (spectrum A, figure 3). This is not surprising; to produce seed wavelengths shorter than 2250 nm, oscillator wavelengths longer than 1000 nm are needed, subject to the phase matching condition imposed by our PPLN crystal. However, the ‘red’ end of the oscillator spectrum, above 1 μm , is energy deficient in our case, as is evident from figure 1(b).

Spectra B and C in figure 3 have a peculiar ‘flat-top’ shape. Since the experimental setup was directly exposed to the atmosphere, we assume that this shape is a consequence of the absorption of the amplified signal by water vapor (and by carbon dioxide) in the air. This absorption leveled off the otherwise rising, beyond 2.4 μm , spectral intensity signal. The sharp spikes in the 2530 nm–2600 nm spectral region, where water vapor absorbance is prominent, indicate a significant energy content of the longer-wavelength edge of spectra B and C prior to the atmospheric absorption. Therefore, it is reasonable to expect that not only the absolute amplitude but also the width of spectra B and C, will be increased by reducing the amount of water vapor in the air, in the vicinity of the setup, by purging it with dry nitrogen. Interestingly, the width of the C spectrum is more than 200 nm even without purging. It was difficult to assess its true extent because spectral measurements deeper in the IR were inhibited by the sharp drop in responsivity of the PDA10D InGaAs detector, at wavelengths longer than 2.6 μm .

To directly confirm that the output contains ultrashort pulses, a second-harmonic interferometric autocorrelation of the signal was conducted in a non-linear crystal (0.1 mm thick LNB, Eksma). The trace is presented by the blue line in figure 4. The thick red line in the same figure is the Gaussian fit of the intensity autocorrelation, which was obtained from the interferometric autocorrelation by Fourier filtering the latter. The width of the fit corresponds to a Gaussian intensity

envelope pulse of 87 fs duration (FWHM). According to our calculations, the thin LNB crystal used for the SHG provides sufficient bandwidth for undistorted SH autocorrelation signal.

Since we did not attempt to compensate for the chirp accumulated by the pulse in the various dispersive elements of the setup, it is most likely not FT limited. We base this assumption on the fact that spectrum B, typical for the output for which the autocorrelation was measured, can support shorter pulses. Modeling this spectrum by a Gaussian centered at 2465 nm with a 177 nm FWHM yields a 50.5 fs long transform-limited Gaussian pulse. Should this model pulse traverse our setup, it will accumulate positive as well as negative group delay dispersion (GDD), at its central wavelength. The positive GDD is accumulated by the pulse during its four passes in the Cr:ZnSe crystal (5650 fs^2) and in the air ($\sim 30 \text{ fs}^2$). The negative GDD is accumulated mainly in the RTP crystals of the pulse picker and its polarizers (-4150 fs^2) but also in the 1 mm thick LNB (about -200 fs^2). A 2 mm thick positive CaF_2 lens ($f = 500 \text{ mm}$) was introduced between the second parabolic mirror of the parametric seed generator (PM2 in figure 1(a)) and the pulse picker. Its main purpose was to reduce the divergence angle of the seed beam, but it also introduces -106 fs^2 GDD to the seed pulses. Summing-up the various contributions, the model pulse can accumulate about 1230 fs^2 of total positive GDD, at 2465 nm, in our amplifier. Calculating the length of the thus obtained positively chirped pulse produces 84.3 fs (FWHM), a value that agrees well with the measured length of the actual pulse. The small discrepancy between the two values can be attributed to the limitations of the model, as well as to higher order dispersion terms accumulated by the actual pulse.

In conclusion, we report on a hybrid amplification scheme in which, at the first stage, we generate mid-IR CEP locked seed pulses, around 2.5 μm , through intra-pulse DFG from an 8 fs commercial Ti:sapphire oscillator. At the second stage, the seed is amplified in Cr:ZnSe amplifier which is pumped by a Q-switched Tm:YLF laser. After 4 passes in the amplifier, we attain pulse energy of ~ 1.1 nJ and pulse duration of ~ 87 fs at a repetition rate of 1 kHz. This amplification strategy combines the simplicity of laser amplifiers with the advantage of passive CEP stabilization of OPAs. It was repeatedly shown in various parametric and laser amplification schemes that the CEP is faithfully preserved in the amplification process [15, 34]. Moreover, broadband Ti:sapphire oscillators are nowadays widespread and available in many laboratories. Therefore, with additional multipass amplification, this hybrid laser system could be a relatively cheap and simple source of ultrashort CEP stabilized pulses with central wavelength at $\sim 2.5 \mu\text{m}$, obviating the need to operate a dedicated, actively CEP stabilized mid-IR oscillator.

Acknowledgment

This research is supported by the Israeli Ministry of Science, Technology, and Space (53998) and the Wolfson Foundation.

References

- [1] McPherson A, Gibson G, Jara H, Johann U, Luk T S, McIntyre I A, Boyer K and Rhodes C K 1987 *J. Opt. Soc. Am. B* **4** 595–601
- [2] Midorikawa K 2011 *Japan. J. Appl. Phys.* **50** 090001
- [3] Hentschel M, Kienberger R, Spielmann C, Reider G A, Milosevic N, Brabec T, Corkum P, Heinzmann U, Drescher M and Krausz F 2001 *Nature* **414** 509–13
- [4] Sansone G et al 2006 *Science* **314** 443–6
- [5] Drescher M, Hentschel M, Kienberger R, Uiberacker M, Yakovlev V, Scrinzi A, Westerwalbesloh T, Kleineberg U, Heinzmann U and Krausz F 2002 *Nature* **419** 803–7
- [6] Deng Y, Zeng Z, Jia Z, Komm P, Zheng Y, Ge X, Li R and Marcus G 2016 *Phys. Rev. Lett.* **116** 073901
- [7] Corkum P B 1993 *Phys. Rev. Lett.* **71** 1994
- [8] Krause J L, Schafer K J and Kulander K C 1992 *Phys. Rev. A* **45** 4998
- [9] Lewenstein M, Balcou P, Ivanov M Y, L’Huillier A and Corkum P B 1994 *Phys. Rev. A* **49** 2117–32
- [10] Marcus G, Helml W, Gu X, Deng Y, Hartmann R, Kobayashi T, Strueder L, Kienberger R and Krausz F 2012 *Phys. Rev. Lett.* **108** 023201
- [11] Tate J, Augustine T, Muller H G, Salieres P, Agostini P and DiMauro L F 2007 *Phys. Rev. Lett.* **98** 013901–4
- [12] Colosimo P et al 2008 *Nat. Phys.* **4** 386–9
- [13] Marcus G, Zigler A, Englander A, Katz M and Ehrlich Y 2003 *Appl. Phys. Lett.* **82** 164–6
- [14] Marcus G, Zigler A, Eger D, Bruner A and Englander A 2005 *J. Opt. Soc. Am. B* **22** 620–2
- [15] Gu X et al 2009 *Opt. Express* **17** 62–9
- [16] Fuji T, Ishii N, Teisset C Y, Gu X, Metzger T, Baltuska A, Forget N, Kaplan D, Galvanauskas A and Krausz F 2006 *Opt. Lett.* **31** 1103–5
- [17] Cerullo G, Baltuska A, Mücke O D and Vozzi C 2011 *Laser Photon. Rev.* **5** 323–51
- [18] Keller U 2004 Ultrafast solid-state lasers *Progress in Optics* vol 46 (Amsterdam: Elsevier) pp 1–115
- [19] Fermann M E and Hartl I 2013 *Nat. Photon.* **7** 868–74
- [20] Duval S, Bernier M, Fortin V, Genest J, Piché M and Vallée R 2015 *Optica* **2** 623–6
- [21] Demirbas U, Schmalz M, Sumpf B, Erbert G, Petrich G S, Kolodziejewski L A, Fujimoto J G, Kärtner F X and Leitenstorfer A 2011 *Opt. Express* **19** 20444–61
- [22] Ripin D J, Chudoba C, Gopinath J T, Fujimoto J G, Ippen E P, Morgner U, Kärtner F X, Scheuer V, Angelow G and Tschudi T 2002 *Opt. Lett.* **27** 61–3
- [23] Chudoba C, Fujimoto J G, Ippen E P, Haus H A, Morgner U, Kärtner F X, Scheuer V, Angelow G and Tschudi T 2001 *Opt. Lett.* **26** 292–4
- [24] Payne S A and Krupke W F 1996 *Opt. Photon. News* **7** 31–5
- [25] Sorokina I T, Sorokin E and Carrig T 2006 Femtosecond pulse generation from a SESAM mode-locked Cr:ZnSe laser *Conf. on Lasers and Electro-Optics/Quantum Electronics and Laser Science Conf. and Photonic Applications Systems Technologies (2006)* (Washington, DC: Optical Society of America) p CMQ2 (<https://doi.org/10.1109/CLEO.2006.4627853>)
- [26] Sorokina I T and Sorokin E 2007 Chirped-mirror dispersion controlled femtosecond Cr:ZnSe laser *Advanced Solid-State Photonics (2007)* (Washington, DC: Optical Society of America) p WA7 (<https://doi.org/10.1364/ASSP.2007.WA7>)
- [27] Tolstik N, Sorokin E and Sorokina I T 2014 *Opt. Express* **22** 5564–71
- [28] Vasilyev S, Moskalev I, Mirov M, Mirov S and Gapontsev V 2015 *Opt. Lett.* **40** 5054–7
- [29] Schliesser A, Picqué N and Hänsch T W 2012 *Nat. Photon.* **6** 440–9
- [30] Potemkin F V et al 2016 *Laser Phys. Lett.* **13** 015401
- [31] Potemkin F V, Migal E A, Pushkin A V, Sirotkin A A, Kozlovsky V I, Korostelin Y V, Podmar’kov Y P, Firsov V V, Frolov M P and Gordienko V M 2016 *Laser Phys. Lett.* **13** 125403
- [32] Potemkin F V et al 2017 Gigawatt mid-IR (4–5 μm) femtosecond hybrid Fe^{2+} :ZnSe laser system *Proc. SPIE* **10238** 102380L
- [33] Korenfeld A, Sebbag D, Ben-Ami U, Shalom E, Marcus G and Noach S 2015 *Laser Phys. Lett.* **12** 045804
- [34] Langdon B et al 2015 *Opt. Express* **23** 4563–72